Macroscopic Simulation of Multi-axis Machining Processes

Meysam Minoufekr[1], Lothar Glasmacher[1] and Oliver Adams[2]
[1]*CAx-Technologies, Fraunhofer-Insitute for Production Technology, Steinbachstr. 17, 52074 Aachen, Germany*
[2]*Chair of Manufacturing Technology, WZL, RWTH Aachen University, Steinbachstr. 19, 52074 Aachen, Germany*

Keywords: Geometric Modelling, NC Machining Simulation, Tool/Workpiece Engagement.

Abstract: The machining of safety-critical components, e.g. turbine disks and blades, is expected to meet highest demands regarding functionality and quality. At the same time, a fast and affordable process design for the production is a major driver for the economic development of these components. Effective increase in productivity requires in addition to the development of machining technologies, new approaches in process design and planning. The integration of simulation into computer aided design of multi-axis processes provides a great potential for further optimisation of the processes. By using the macro simulation model introduced in this paper, the computational complexity to gain relevant process information is reduced and hence made accessible more easily. Through the presented macro simulation, detailed tool-workpiece engagement is calculated which co-relates to mechanical and thermal stresses on the tool. Based on the calculations the process can be designed by reducing the tool load in the course of the process. This way, the tool life of the used milling cutters can be significantly increased resulting in an increase of process robustness and efficiency, thereby reducing used resources.

1 INTRODUCTION

The process sequence for milling of free-form surfaces can be divided into roughing, pre-finishing and finishing. When roughing, the goal is often to achieve a high performance cutting process (HPC) by driving the process at maximal feed rates and depth of cut resulting in a high material removal rate (MRR). However, in HPC processes high feed rates lead to increasing cutting forces and tool loads which have to be controlled in order to avoid a large tool wear or even tool breakage during the process. The workpiece resulting from the roughing operation is usually characterized by a macroscopic surface roughness on the surface contour, (Arntz, 2013). In pre-finishing, a uniform surface is achieved by removing the rest material generated in the rough machining. The goal of pre-finishing is a constant material distribution on the entire workpiece, so that in the following finishing operation, requirements of accuracy and surface quality can be achieved. As the last process, finishing is critical since the final surface of the part is generated. Failures in finish milling lead to expensive rework or even to scrap generation. Both, in pre-finishing and in the subsequent finishing processes, often a high speed cutting (HSC) approach is applied by using extremely high spindle speed and feed rates. In the course of HSC processes, the engagement conditions, e.g. the contact angle and the resulting chip thickness, have to be controlled since, in combination with the cutting speeds, the mechanical and thermal loads on the tool may result in low surface quality on the final part. Consequently, in HPC as well as in HSC processes, methods are needed for a careful process design to drive the processes to their limits but also to avoid critical situations along the value chain of the processes.

Especially in the transition from roughing to pre-finishing, the analysis and evaluation of the engagement conditions plays an important role, as the contact situation between cutter and workpiece becomes unpredictable. The residual material geometry on the workpiece, which results from roughing, usually cannot be determined in advance for parts with free-form geometry. Contact situations of the tool and the workpiece leading to unknown and possibly undesirable engagement conditions seem to be unavoidable during the process. Due to the continuously changing machining allowance and contact situation, it is important for the process

Minoufekr M., Glasmacher L. and Adams O..
Macroscopic Simulation of Multi-axis Machining Processes.
DOI: 10.5220/0004631905050516
In *Proceedings of the 10th International Conference on Informatics in Control, Automation and Robotics* (ICINCO-2013), pages 505-516
ISBN: 978-989-8565-71-6

planner to understand the interaction between the tool and the workpiece and evaluate the same against significant process parameters. In particular, the engagement conditions during simultaneous five-axis milling have to be observed in this context.

The simulation approach introduced in this work helps to understand the geometrical engagement situation occurring in the milling process. Thus, critical regions in the process where engagement condtions exceed the tolerances can be automatically identified, Figure 1. This is the basis for a process analysis, since process parameters directly related to the geometrical engagement conditions are evaluated and optimised in advance.

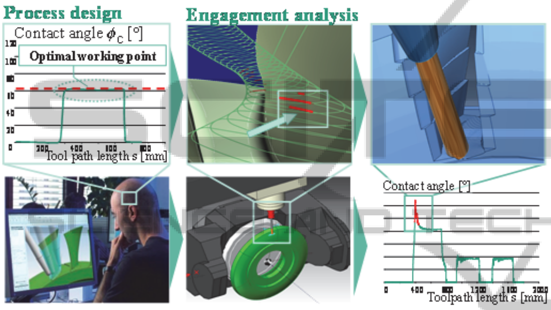

Figure 1: General idea for simulation of critical sections on the toolpath.

So, this paper suggests the macro simulation model for multi-axis machining processes. It is structured as follows. In section 2, problems in current multi-axis machining are described. Furthermore, the engagement and fundamental parameters defining the cutter-workpiece contact are analysed. In section 3, the macroscopic simulation model for machining processes is introduced. Based on this concept, the calculation models for discrete engagement conditions are explained in-depth. Then, in section 4 the macro simulation is discussed by a roughing example, where engagement conditions are calculated. The paper is finally concluded in section 5.

2 BACKGROUND AND PROBLEM DEFINITION

Almost any complex part can be produced using simultaneous multi-axis machining. Here, the simultaneous multi-axis milling is characterized by suddenly changing the tool orientation and the transient contact conditions between tool and workpiece. The manufacturing of the parts is carried out on NC controlled machine tools. Here, the process is loaded as a series of NC commands, i.e. the "NC program", on the machine tool and executed. Depending on the NC command in the NC program, up to three translational and two rotational axes are controlled simultaneously during the machining. Accurate NC programs are crucial for manufacturing without interruption and potential machine breakdowns. Due to the complex kinematics, milling processes are not verifiable without supporting process design tools because it is difficult to visualise the location of the cutting tool due to the complex axis control. The consequences are unpredictable and probably critical to cutting conditions, Figure 2.

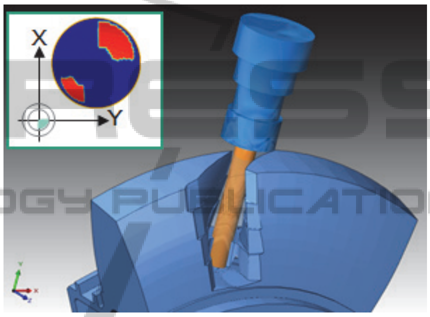

Figure 2: Example of a BLISK manufacturing with a critical engagement due to collision of the workpiece with the non-cutting part of the cutter.

Nowadays, the development of machining processes is characterized by a sequential iterative approach, which has to be followed in a few optimization loops before reaching stable production, (Schug, 2012). Therefore, computer based technologies (CAx technologies) are involved in planning and verification of the entire milling process in advance, Figure 3. The parameter windows and the acquired technology knowledge gained from machining trials are used to determine the process-specific, optimal parameter combinations which are essential in the design and planning of the manufacturing.

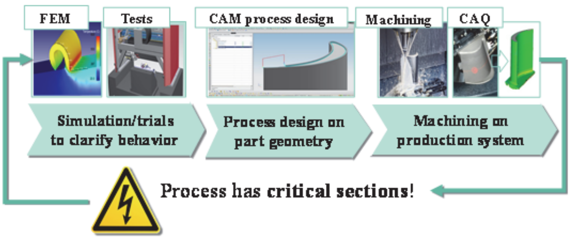

Figure 3: Sequential CAx process chain for machining.

The planning in CAM is dedicated to the design of the machining operation where the milling toolpath is parameterized by process variables such as cutting speed and depth of cut to manufacture the real part geometry. The designed process is transferred to the production system by an appropriate output data format for machining. Potential errors that are identified at the end of the process design stage, or during the process carried out on the machine tool, cause expensive iteration steps. According to (Zabel, 2010), the costs to eliminate an error increase with the progress of the process design stages. Consequently, an identification of process parameters leading to undesired cutting conditions is considered necessary at an early stage in the process planning.

2.1 Simulation-based Design of Multi-axis Processes

The main application of process simulation is in the area of computer-based process planning and design, Figure 4. By using the process simulation, it is possible to locate errors and fix problems faster, than it is achievable through trial-and-error methods. The starting point for using the process simulation system is between the NC data generation by the CAx system and the loading of NC data on the machine tool. Unlike the sequential CAx process chain, the NC data is not transferred directly to the machine tool, but passed to the simulation system. Especially requirements referring to the efficiency of the used simulation tool process play a role because the simulation increases the CAx process design chain length, (Zabel, 2010). In this context, the simulation model with affordable complexity of computation time and space is desirable.

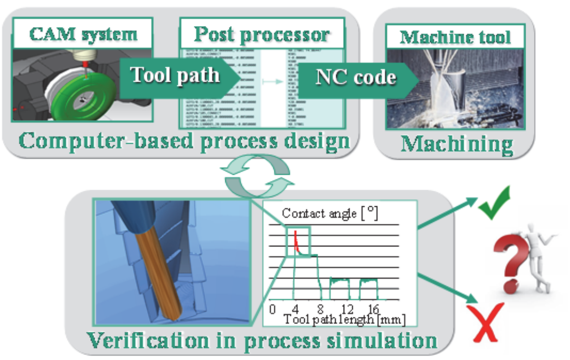

Figure 4: Evaluation of the process behaviour by the presented simulation approach.

2.2 State of the Art in the Simulation of Machining Processes

Numerous simulation approaches have been developed in the last decades with the objective of determining the important parameters of the machining process which can be classified as FE-based models, analytical models and geometrical models, Figure 5. The group of geometrical models can be further subdivided into approaches using constructive solid geometries (CSG) and spatial space partitioning schemes. Zabel gives a detailed overview of these models and their application in (Zabel, 2010).

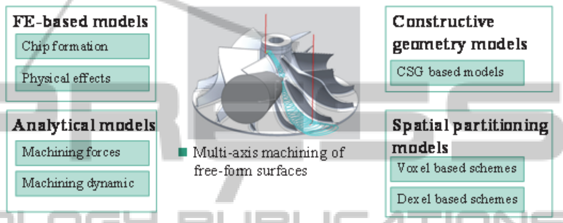

Figure 5: Overview of existing simulation models for machining processes.

Although many physical effects can be modeled by using FEM and analytical model equations, however, the predictive capabilities of available approaches are still limited and thus cannot be applied for planning the entire multi-axis operation. A complete analysis of five-axis milling processes, i.e. simulation of every instant of the process is expensive due to limitations on available computing capacity and hardly practical. On the other hand, geometric models focus on the determination of visual properties such as the shape of the workpiece during the milling operation by efficient real-time methods for updating the workpiece.

Simulation techniques based on the discretization of the workpiece vary according to the geometric design, (Glaeser, 1997), (Jerard, 1989), (Robert, 1987). Milling simulation methods based on the voxel or dexel model are presented in (Ayasse, 2001) and (Stautner, 2005). The consideration of physical properties is of minor importance. Systems like *Vericut* offer simulation methods for collision detection in three and five axis milling, (CGTech, 2013). The adjustment of the NC programs is often based on parameters, wherein the simulated residual material on the finished part is used to increase the material removal rate. However, only the feed rates are adjusted, the geometry of the toolpath remains unchanged. In these systems, assumptions in the modeling approaches are highly simplified. Hence, results obtained are insufficient for a qualitative statement about the geometrical engagement situation in the course of the milling process.

2.3 Macroscopic Engagement Conditions for Process Evaluation

The mechanical and thermal tool load is primarily dependent on the combination of three factors: the chip thickness h_{sp}, the contact angle ϕ_c and the contact length l_{sp}, Figure 4.

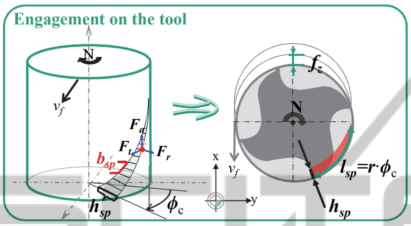

Figure 6: Engagement of cutting tool at instant t.

Optimal cutting conditions can be maintained easily in straight cuts by constant cutting width a_e. However, engagement situations change rapidly in a multi-axis process. In machining of free-form surfaces, the contact angle ϕ_c increases, whenever the tool enters a turn causing a longer contact length l_{sp} between the cutting edges and the workpiece, Figure 7. In fact, cutting-edge temperature increases significantly as the contact length l_{sp} increases, which results in a decrease of tool life. This relation has been proven by Meinecke in (Meinecke, 2009).

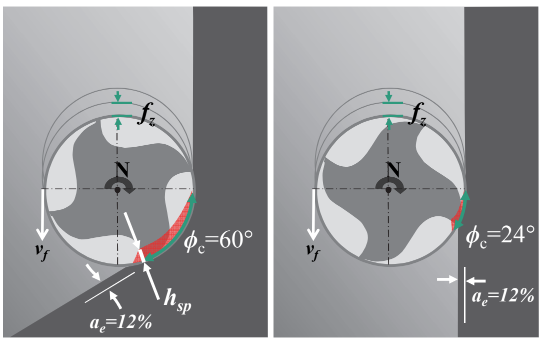

Figure 7: Straight vs. corner cuts result in different engagement despite equal cutting depth, (Diehl, 2011).

The relevance of the contact angle ϕ_c can also be seen in cutting theory, as the chip thickness h_{sp} increases with increasing ϕ_c and thus leads to higher cutting forces, (Klocke, 2011). According to Ståhl, (Ståhl, 2012), the approximate chip thickness h_{sp} and the chip width b_{sp} are expressed by the contact angle ϕ_c and the axial depth of cut a_p, respectively:

$$h_{sp} \approx f_z \cdot sin\,\phi_c \quad (1)$$

$$b_{sp} \approx \frac{a_p}{\sin\kappa} \quad (2)$$

where κ is the major cutting edge angle of the cutting tool, f_z the feed per tooth and a_p the cutting depth. Specifically, the the machining forces in radial (F_r), tangential (F_t) and axial direction (F_a) are related to the contact angle ϕ_c. This can be seen by substituting h_{sp} and b_{sp} in the Kienzle equation, (KLocke, 2011):

$$F_i = \frac{a_p}{\sin\kappa} \cdot k_{i1.1} \cdot (f_z \cdot \sin\phi_c)^{(1-m_i)} \quad (3)$$

where $k_{i1.1}$ and m_i are material specific constants and $i \in \{a,r,t\}$. Hence, the contact angle and the contact length play a major role in the evaluation of machining processes. For the calculation of the contact angle ϕ_c, it is necessary to regard the cutter-workpiece engagement at each point in time in the course of the process. However, the contact angle can be determined by considering the interaction of the tool bounding geometry with the workpiece, where the angular contact area on the tool is referred as $\phi_c = \phi_{ex} - \phi_{st}$, i.e. defined as the difference of the exiting angle ϕ_{ex} and the starting angle ϕ_{st}, Figure 8. In accordance to (Meinecke, 2009), quantities as ϕ_{ex} and ϕ_{st} are referred to as macro conditions, since their calculation is abstracted from the exact tool geometry and the tool cutting edges are not taken into account.

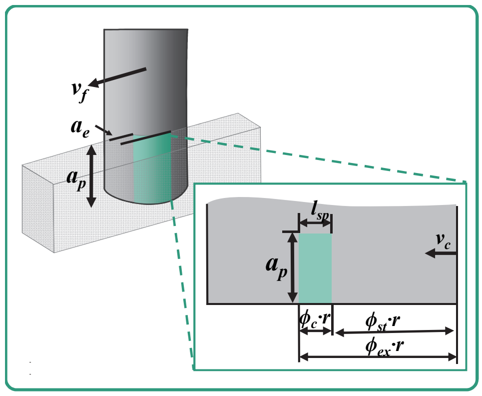

Figure 8: Macro engagement of cutting tool.

2.4 Influence of the Tool Geometry and Tool Kinematic

In addition to the suddenly changing contact situation in the course of the multi-axis milling, two further aspects complicate the calculation of macro conditions at each instant of the process; the tool geometry and tool orientation. During the machining of freeform surfaces many constellations of the engagement may arise from the material removal leading to sudden changes of engagement conditions along the tool.

To capture the engagement situation in multi-axis machining, an extended definition of process parameters and engagement conditions is needed considering the tool geometry and the tool orientation. Hence, the engagement conditions are parameterized by their axial location $k \in [0,l]$ on the tool axis at an instant in the course of the process. Thus, the starting and exiting angle are defined as $\phi_{st}(k)$ and $\phi_{ex}(k)$, respectively. Also the radial depth of cut is referred to the current location of the tool axis and is deified as $a_e(k)$. Since the tool radius is also variable along the tool axis it is also parameterized as $r(k)$, Figure 9.

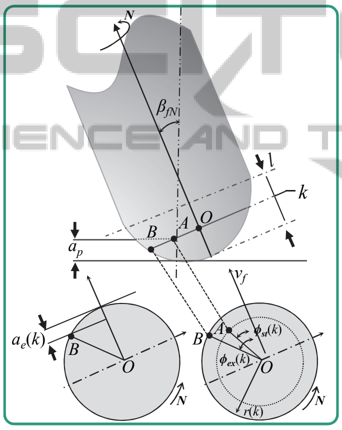

Figure 9: Parameterization of the engagement conditions in reference to the tool length l.

When machining with ball end mills, for instance, every cutter point undergoes a different load during the engagement. The altering contact along the tool axis has consequences for the determination of the chip length l_{sp}, since it depends on the contact angle ϕ_c and tool radius $r(k)$ which is varying according to the tool shape along the tool axis, Figure 10.

The calculation of the engagement condition is further complicated by the orientation of the tool relative to the workpiece and the feed direction. In context of NC machining, the position of the tool is defined by a local tool coordinate system TCS which has its origin at the tool center point $\boldsymbol{O}_{TCS}$ and is determined by the current feed direction v_f, the tool orientation n and the bi-normal $b = n \times v_f$, Figure 11. The orientation of the tool vector n is determined by the lead and tilt angle β_{fN} and β_N, respectively.

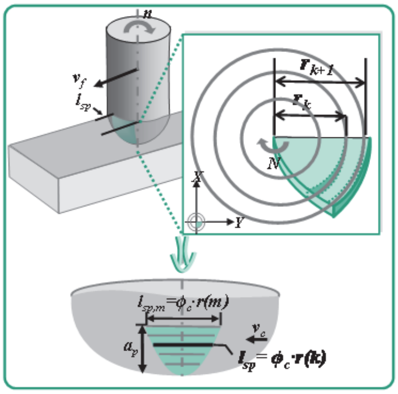

Figure 10: Influence of the tool geometry on the calculation of engagement conditions.

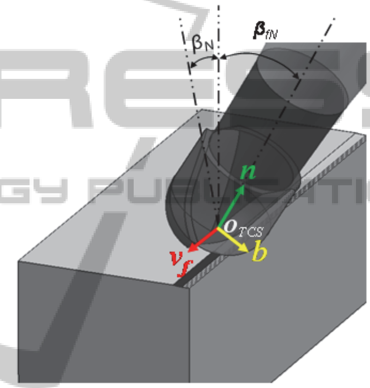

Figure 11: Definition of the Tool coordinate system.

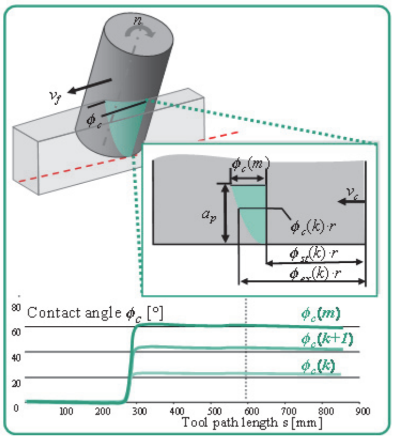

Figure 12: Influence of the tool orientation on the engagement conditions.

During the machining of freeform surfaces, the tool may be tilted to the surface normal, i.e. $\beta_N \neq 0$ and $\beta_{fN} \neq 0$, respectively. Since the contact situation depends on the lead angle β_N and tilt angle β_{fN}, describing the angular situation of the tool normal vector n to the surface of the workpiece, (Arntz, 2013), the starting and exiting angles $\phi_{st}(k)$ and $\phi_{ex}(k)$ vary along the tool axis resulting from the kinematic situation of the tool and the workpiece. Hence, at each individual tool height, there is a different contact angle $\phi_c(k)$, Figure 12. Depending on the tool orientation to the workpiece, the contact angle $\phi_c(k)$ varies along the tool axis at a discrete instant *t*.

2.5 Problem Definition and Research Question

On one hand, the engagement situation depends on the orientation resulting in altering contact angles $\phi_c(k)$ along the tool axis. This affects also the course of h_{sp}, which is followed by equation (2). On the other hand, the tool geometry, in particular the variable tool radius along the tool axis leads to changing contact lengths during the engagement. Additionally, the contact situation changes in the course of the cutting process at each instant *t*. Thus, the contact angle on the tool is defined as $\phi_c(t,k)$ specifying the angular contact on point $k \in [0,l]$ along the tool axis and at an arbitrary point in time *t*. Furthermore, the contact length can be expressed as

$$l_{sp}(t,k)= \phi_c(t,k) \cdot r(k) \qquad (4)$$

In this context, the following assumption can be formulated:

A discretized simulation model allows a sufficiently accurate approximation of macroscopic engagement conditions in the course of multi-axis machining processes.

To verify this key assumption, the following research question has to be investigated:

Can the geometrical contact situation of multi-axis machining processes be described as a sequence of discrete states, where engagement conditions vary on each discrete point k on the tool axis and at each discrete instant t?

Answering this question involves the realization of a simulation model which allows a sufficiently accurate approximation of geometrical engagement conditions, in particular macroscopic engagement conditions, between the cutting tool and the workpiece in simultaneous multi-axis machining.

3 SOLUTION AND METHOD

The geometrical simulation approach introduced in this paper, determines macroscopic engagement conditions by regarding the cutter-workpiece engagement area based on a discretized geometry model. The macro simulation is based on a hierarchical simulation approach which allows the prediction of engagement conditions on the tool over a sufficiently long period of time by purely geometrical modelling, Figure 13. Based on the macroscopic simulation, critical process areas can be identified or can be investigated for sub-optimal process performance.

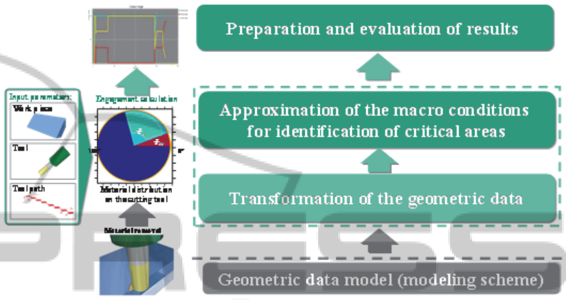

Figure 13: Hierarchical structure of the simulation system for macroscopic engagement conditions.

Therefore, the toolpath is divided into discrete segments. At each discrete point on the toolpath, the contact between the tool and the workpiece geometry is determined and then used for calculating the engagement conditions, Figure 14. Between two points on the toolpath, the intersection of the bounding geometry of the tool and the workpiece model is determined. The set of intersecting points can be used directly for the calculation of removed material on the workpiece model. The removed material data resulting from the tool position and orientation on the current toolpath point is used to derive the macro conditions, i.e. the contact angle $\phi_c(t,k)$ and the chip length $l_{sp}(t,k)$. At a discrete instant *t* of the process, the profile of macroscopic quantities can be determined along the tool axis by subdividing the tool in m+1 tool discs, resulting in a particular value $\phi_c(t,k)$ at each tool disc *k*, where k=0,1,2,… m.

Since the calculation of macro conditions is abstracted from the exact cutting geometry, the computational effort is drastically reduced. So, macroscopic conditions are calculable throughout the entire process by avoiding expensive calculation steps. Both aspects, namely sufficient reliability of the model as well as demands on efficiency are achieved. In this regard, efficient techniques for workpiece update with special consideration of a sufficiently precise engagement modeling are indispensable. Especially complex workpiece geometries with machining operations consisting of several 100,000 NC blocks need to be verified in the macro simulation with the reasonable response times.

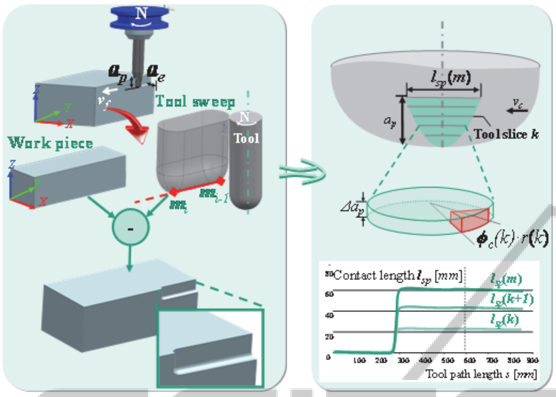

Figure 14: Geometric approach for macroscopic engagement simulation of multi-axis processes.

3.1 Calculation Models for Macro Simulation

The calculation of engagement conditions is based on the geometrical contact of the cutter and the workpiece. Accurate predictions on the contact between the tool and workpiece are the basis for further calculations and therefore essential in the simulation approach. Both the tool and the workpiece can be modeled in the context of geometrical simulation in various ways. Highly dimensioned and complex workpiece geometries require a large memory usage and fast methods for the update during machining. So, the choice of appropriate "modeling schemes", i.e. how a workpiece is discretized, (Stifter, 1995) affects the simulation accuracy and space complexity greatly, Figure 15.

A further focus is on the introduction of modeling schemes with special consideration of a sufficiently accurate mapping of engagement conditions since engagement calculations are directly derived from the discretized elements of the workpiece model and hence influence the quality of the simulation results. Practical tests have shown that the dexel and the multi-dexel scheme provide a high accuracy for engagement calculation operations while allowing an efficient dynamic update of the workpiece, Figure 16.

The workpiece model representation used in this work is based on the multi-dexel scheme introduced by Stautner, (Stautner, 2005). Furthermore, the boundary model of the milling tool, given as a CSG model, is used to determine the contact area, i.e. the cutting edges of the tool are neglected. The dexel scheme is an instance of spatial enumeration techniques with desired requirements referring accuracy and performance, (Stifter, 1995).

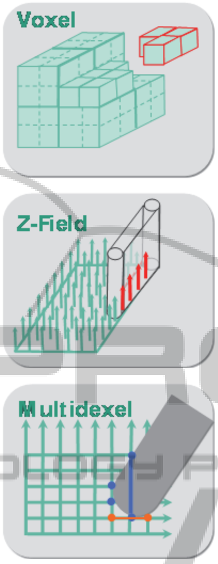

Cubic memmory usage of the Voxel model, $O(n^3)$

Cube size	Memmory usage
128x128x128	8MB
256x256x256	64MB
512x512x512	512MB
1024x1024x1024	**4096 MB**

Quadratic memmory usage of the Z-Field model, $O(n^2)$

Cube size	Memmory usage
128x128x128	4MB
256x256x256	16MB
512x512x512	64MB
1024x1024x1024	**256MB**

Quadratic memmory usage of the Multi-Dexel model, $3O(n^2)$

Cube size	Memmory usage
128x128x128	4MBx3=12MB
256x256x256	16MBx3=48MB
512x512x512	64MBx3=192MB
1024x1024x1024	256MBx3= **768MB**

Figure 15: Space complexity of the modelling schemes and their memory usage for a cube geometry.

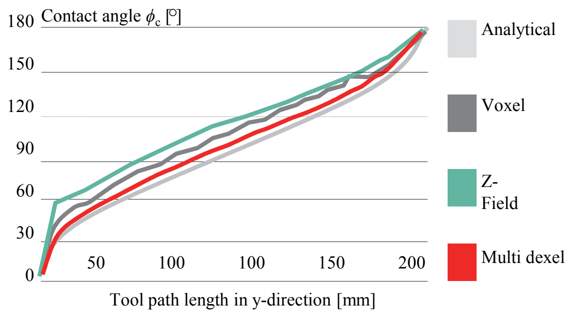

	Nominal	Δ Z-Fiels	Δ Voxel	Δ Multidexel
Max. Error	137.54°	10.64°	14.83°	4.23°
Ø Error	0.00°	6.77°	8.23°	2.7°

Figure 16: Accuracy of the modelling schemes for engagement calculation.

The dexel model of the workpiece is determined by a set of parallel and equidistant rays intersected with the original workpiece geometry, Figure 17. By intersecting each ray with the workpiece, two points on a line segment, which is totally inside the workpiece, are determined. A dexel is defined by these two points on the line segment. The intersection points can be calculated with a high accuracy since the dexel grid provides float precision parallel to the ray direction. However, a single dexel model leads to deviations in representing the original workpiece if the shape is sampled parallel to the projection plane of the dexel grid. Here, the determination of intersection is depending on the grid interval.

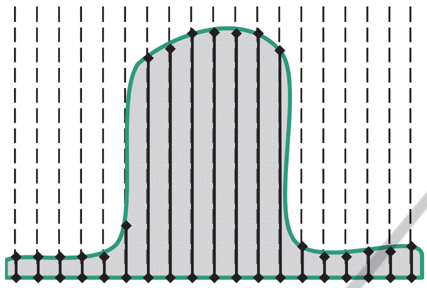

Figure 17: Dexel based representation of the workpiece.

To overcome this insufficiency, the multi-dexel scheme is used which can be regarded as an extension of the dexel model. As shown in Figure 18, the multi-dexel model consists of three overlapping orthogonal dexel grids. Compared to the single direction dexel model, the multi-dexel scheme expresses a model more precisely since the computation of each coordinate of an intersection point can be performed with float precision. The multi-dexel model is defined as a set of $\{d_{i,j,k}\}$, by a constant grid distance δ relative to the origin point $\boldsymbol{O}$, (Ren, 2008). Each dexel $d_{i,j,k}$ has two nodes $\xi^{l}_{i,j,k}$ and $\xi^{u}_{i,j,k}$ as the lower and the upper bound of the dexel segments, Figure 18. The space complexity is estimated by $O(N_x{\cdot}N_y + N_y{\cdot}N_z + N_x{\cdot}N_z){\cdot}M_d \in O(N^2)$, where N_i are the cell numbers along principal axes and M_d is the maximum number of dexel nodes.

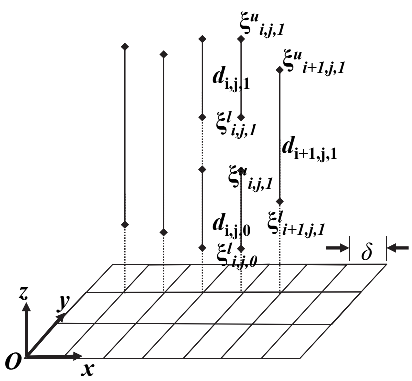

Figure 18: Logical structure of the dexel model, (Ren, 2008).

To simulate the material removal by machining, the contact area between the tool and dexels that are involved in the cutting are calculated at a given instant. This means a rearranging of the dexel data at region of tool-workpiece interaction, while the entire material removal requires a sequential update of the dexel elements. These steps are repeated at each discrete point of the machining toolpath until the machining process is completed, Figure 19.

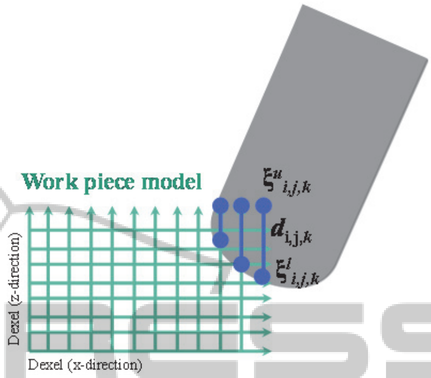

Figure 19: Intersection of the tool with the workpiece.

3.2 Calculation of Macroscopic Engagement Conditions

The contact between the tool and the workpiece can be calculated by the intersection of the tool boundary geometry and the dexels. This requires determining the area of the tool that is in contact with each dexel and then identifying the corresponding $\xi^{l}_{i,j,k}$ and $\xi^{u}_{i,j,k}$ for each $d_{i,j,k}$ involved during a cut. Hence, let S_{Tool} and $S_{Workpiece}$ be defined as the tool domain and the workpiece domain, respectively. Further, let $p=(p_x,p_y,p_z) \in S_{Tool}$ be a discrete point of S_{Tool} and $q=(q_x,q_y,q_z) \in S_{Workpiece}$ be a point on the workpiece. If the condition

$$\exists\ \alpha,\beta,\gamma \in \{i,j,k\} \text{ with } p_\alpha \leq q_\alpha,\ p_\beta = q_\beta,\ p_\gamma = q_\gamma, \quad (5)$$

is satisfied at a discrete point in time t, the tool and the workpiece are considered to be in engagement and lead to the engagement domain $D(t)$, which is defined as follows:

$$D(t) = \{(s^l, s^u) \mid s^l \in \mathbb{R}^3, s^u \in \mathbb{R}^3\}, \quad (6)$$

where $s^l=(s^l_x,s^l_y,s^l_z)$ and $s^u=(s^u_x,s^u_y,s^u_z)$ fulfill (5) for a $q \in S_{Tool}$. The set $D(t)$ consists of point pairs describing the line segments which are cut by the tool at t. The corresponding points of the 2-tupels in $D(t)$ can be expressed as $s^l=(i,j,\xi^l_{i,j,k})$ and $s^u=(i,j,\xi^u_{i,j,k})$, respectively by regarding the intersection of the cut dexel $d_{i,j,k}$ and S_{Tool} in the nodes $\xi^l_{i,j,k}$ and $\xi^u_{i,j,k}$, Figure 20.

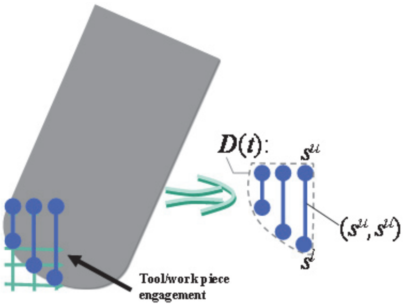

Figure 20: Set of the the intersecting dexel segements with the tool during the engagement.

To express the contact conditions referring to the cutting area on the tool, each element of $D(t)$ is transformed into the coordinate system of the tool TCS, see section 2.4. Thus, the engagement domain $D_{TCS}(t)$ is defined as

$$D_{TCS}(t) = \{(\dot{s}^l, \dot{s}^u) \mid \dot{s}^l = T \cdot s^l - v,\ \dot{s}^u = T \cdot s^u - v\}, \quad (7)$$

where $s^l \in D(t)$, $s^u \in D(t)$ and $T \in \mathbb{R}^{3\times3}$ defined as the basis transformation matrix build up by the three vectors $\boldsymbol{n}$, v_f, $b \in \mathbb{R}^3$. The vector $v \in \mathbb{R}^3$ describes the offset between $\boldsymbol{O}$ and $\boldsymbol{O}_{TCS}$. Furthermore, it can be easily seen that $D_{TCS}(t)$ is bounded by the bounding geometry of the tool, i.e.

$$\forall\ (\dot{s}^l, \dot{s}^u) \in D_{TCS}(t){:}\ (\dot{s}^l, \dot{s}^u) \subseteq S'_{Tool}, \quad (8)$$

where $S'_{Tool} := \{T \cdot q - v \mid q \in S_{Tool}\}$. The macroscopic engagement conditions are derived by using the engagement domain $D_{TCS}(t)$ at each instant t. As described in section 2.5, the contact conditions may vary along the tool axis. In order to estimate the course of engagement conditions depending on the tool axis, the engagement area is evaluated by discretizing the tool along its length in m+1 discs, Figure 21.

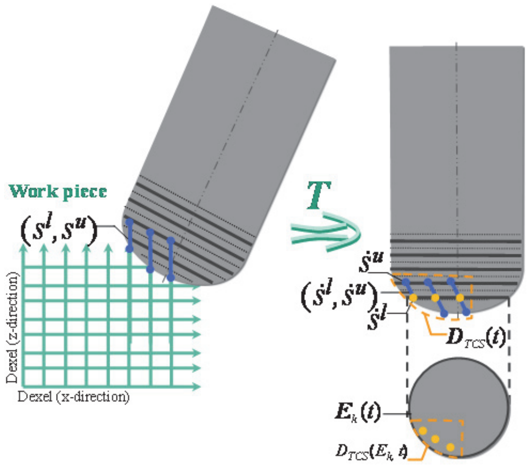

Figure 21: Material removal mapped on the discrete tool disc along the tool axis.

Each disc has a position and an orientation on the tool that defines the oblique cutting performed by that disc segment. For a defined tool orientation $n=(n_x,n_y,n_z)$, the tool discs can be defined as a set of planes originated in $\boldsymbol{O}_{TCS}$:

$$\mathbb{E} = \{E_k \subset \mathbb{R}^3 \mid E_k = \{p \in E_k \mid n_x p_x + n_y p_y + n_z p_z = k \cdot \Delta z\}\} \quad (9)$$

where k=0, 1, 2,…, m. The contact area for each tool disc E_k is determined by finding the intersection of a line segments $(\dot{s}^l, \dot{s}^u) \in D_{TCS}(t)$ with E_k. Hence, the engagement area of E_k at a discrete instant t can be described as

$$D_{TCS}(E_k, t) = \{p \mid \exists (\dot{s}^l, \dot{s}^u) \in D_{TCS}(t){:}\ p \in E_k \cap (\dot{s}^l, \dot{s}^u)\}. \quad (10)$$

For each E_k and $(\dot{s}^l, \dot{s}^u)$, it is true that $\|E_k \cap (\dot{s}^l, \dot{s}^u)\| = 1$, i.e. E_k and $(\dot{s}^l, \dot{s}^u)$ intersect only in p, except $(\dot{s}^l, \dot{s}^u)$ completely lies in E_k. By recalling (6), for every $p \in (\dot{s}^l, \dot{s}^u)$ it is also true that $p \in S'_{Tool}$ since p lies on the line segment limited by $\dot{s}^l$ and $\dot{s}^u$. It follows that $D_{TCS}(E_k, t) \subseteq S'_{Tool}$ for some $E_k \in \mathbb{E}$. Looking closer to $D_{TCS}(E_k, t)$, it can be seen that

$$\forall\ p \in D_{TCS}(E_k, t){:}\ \|p - O_{TCS}\| \le r(k) \quad (11)$$

for $r(k) \in \mathbb{R}$ and k=0,1,…m, i.e. the contact points in $D_{TCS}(E_k, t)$ are bounded by the corresponding tool radius at the tool disc E_k.

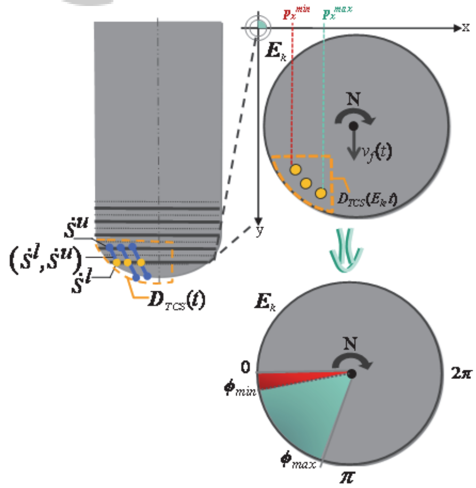

Figure 22: Estimation of the minimal and maximal angles on a tool disc E_k.

The particular angular engagement area for a given disc E_k is given by the minimal angle $\phi_{min}(k)$ and the exit angle $\phi_{max}(k)$ on E_k. These two parameters provide a compact form to describe the tool-workpiece engagement at a particular region along the tool axis at the tool length $l=(m+1)\cdot\Delta z$, Figure 22Figure 23. The minimal angle $\phi_{min}(k)$ and maximal angle $\phi_{max}(k)$ to each respective disc E_k are assigned by finding the point with minimal and maximal coordinates in x-direction on E_k. Thus, let $p^{min}=(p_x^{min},p_y^{min},p_z^{min})$ be the corresponding point to the minimal x-value in $D_{TCS}(E_k,t)$ and $p^{max}=(p_x^{max},p_y^{max},p_z^{max})$ the maximal, respectively. The angular values of $\phi_{max}(k)$ and $\phi_{min}(k)$ are determined by

$$\phi_{min}(k): = \begin{cases} arccos\left(\frac{p_x^{min}}{p_y^{min}}\right), \text{for } p_y^{min} > 0 \\ -arccos\left(\frac{p_x^{min}}{p_y^{min}}\right), \text{for } p_y^{min} < 0 \end{cases} \quad (12)$$

and

$$\phi_{max}(k): = \begin{cases} arccos\left(\frac{p_x^{max}}{p_y^{max}}\right), \text{for } p_y^{max} > 0 \\ -arccos\left(\frac{p_x^{max}}{p_y^{max}}\right), \text{for } p_y^{max} < 0 \end{cases} \quad (13)$$

and $\phi_{min/max}(k):=0$ for $p_y^{min/max}=0$. In case of clockwise rotating tool, it is $\phi_{st}(k)=\phi_{max}(k)$ and $\phi_{ex}(k)=\phi_{min}(k)$. In case of a counterclockwise rotating tool, $\phi_{st}(k)$ and $\phi_{ex}(k)$ are swapped. The contact angle $\phi_c(k)$ at E_k is estimated by $\phi_c(k):=\phi_{ex}(k)-\phi_{st}(k)$, Figure 23.

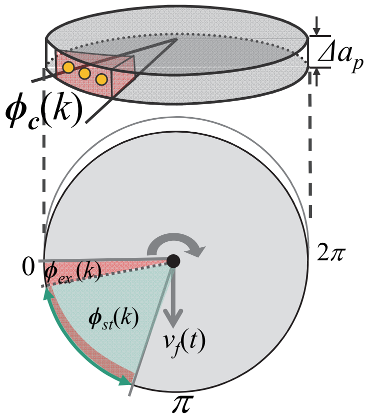

Figure 23: Calculation of contact angle on a tool disc.

4 RESULTS AND DISCUSSION

The main advantage of process simulation is that process behaviour can be evaluated before cost expensive trials are conducted. The link between the simulation with data from the process monitoring results in a higher knowledge base about the process interdependencies in the milling process, Figure 24. Therefore, a synchronisation between both data sources has to be developed. As a synchronisation over time scale is not reliable, because the machine tool's acceleration behaviour has to be known exactly, here an approach using synchronisation over position is chosen.

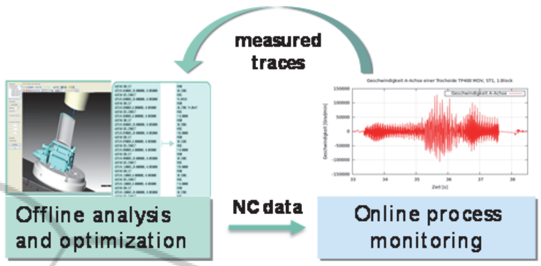

Figure 24: Link between offline and online process analysis.

4.1 Use of the Macro Simulation to Evaluate Processes

In order to prove the concept of linking simulation data with process monitoring data, test geometry is defined and manufactured. The test geometry consists of simple geometric features. A cuboid, a cylinder and a triangle are placed on a rectangular base, Figure 25. As workpiece material Aluminum is used and the tool is a standard 10 mm diameter shaft mill with two cutting edges. The workpiece is mounted on a Kistler 9255B force measurement platform to acquire the process forces. A Mazak Variaxis 630-5X II t, which is a 5-axis machining centre, is used to carry out the experiments.

Table 1: Process setup details and process parameters.

Workpiece	Aluminum 140 mm x 150 mm
Tool	10 mm diameter shaft mill
Cutting parameter	$f_z = 0.1$ mm $v_c = 280$ m/min $a_p = 5$ mm

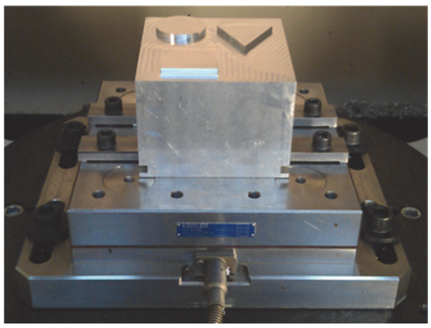

Figure 25: Test setup on Mazak Variaxis 630-5X II t.

The toolpath and CAM operations are conducted in the PLM software Siemens NX 8.5. A standard contour parallel milling strategy is used in combination with conventional cutting, Figure 26.

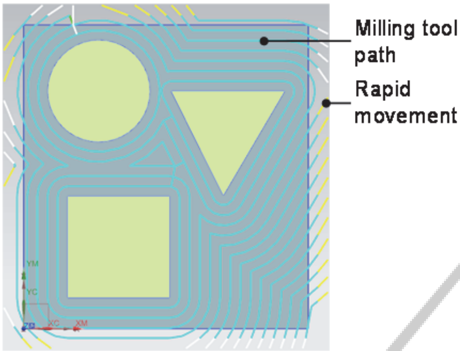

Figure 26: Generated toolpath.

A macro simulation of the engagement condition is carried out and shows the contact angle between workpiece and tool over time, Figure 27. The macro conditions were calculated in 3 sec. 430 ms at a laptop computer (Dell Precision M4600@4x2.2GHz and 8GB RAM). The toolpath was segmented in 2027 discrete points. The workpiece was discretised by a precision $\delta = 0.3$mm. From the simulation it can be seen that the created toolpath leads to frequently changing engagement situations. As the contact angle correlates with the process forces the resulting tool load is varying as well. Critical sections with high contact angle are identified and can be optimized through either changing the toolpath or by reducing the feed rate in the NC program. Furthermore, sections with rather low contact angles can be optimized in order to reduce process time. In addition to optimizing the milling process itself, process monitoring strategies can be applied. Integrating and linking geometric information from macro process simulation with process monitoring tools opens new ways for online-monitoring of multi-axis milling processes.

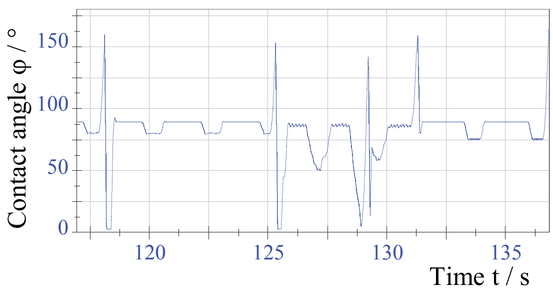

Figure 27: Contact angle over time t.

Using the Kienzle equation, Equation (3), the expected force depending on the local engagement situation is calculated. This allows a process monitoring system to compare online, the expected force with the current force and decide whether the milling process is in a stable situation. Compared to standard monitoring systems no teaching activities are necessary. The result of calculated monitoring force and real process force is evaluated in time domain, Figure 28.

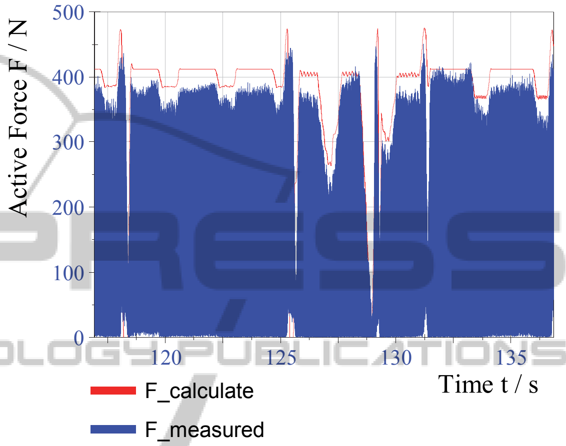

Figure 28: Process monitoring solution for milling process.

5 CONCLUSIONS AND FURTHER RESEARCH

Due to frequently changing manufacturing tasks, it is difficult to control the complexity of machining processes. However, the parts have to be machined with high accuracy, robustness and efficiency. Thus, the shop floors are under strong pressure to deliver optimal results in shorter times.

In order to efficiently find optimal process parameters, the level of production automation for developing processes is important. A simulation approach that allows the determination and evaluation of the actual status of the machine and the process at any time contributes to realize a systematic optimization of machining operations. However, complex calculations are used for the simulation of multi-axis milling processes which are not yet appropriately controllable despite improved hardware technologies and parallelization of algorithms. Important as the use of powerful hardware and parallel algorithms may be, novel concepts are needed to minimize the complexity of the problems to be analysed on the essential level of abstraction.

In this paper, the macro simulation for multi-axis machining processes has been introduced which focusses on significant parameters in the process. It enables the reliable detection of disturbances such as process instabilities or overloads of tool and/or machine which lead to an excess of tolerances and hence undesired process deviations. Thus, the presented work contributes to a significant reduction of expensive damages and system failures in production. Apart from the prediction of engagement conditions, further research is needed to modify process parameters based on the simulation. Complex toolpaths in particular can be optimized regarding the manufacturing and design parameters. The adjustment of feed rates, the toolpath trajectory and the tool definition offer a potential for reducing the process time and creating a more robust machining process. Hence, future research will focus on optimizing these parameters based on macroscopic engagement conditions.

ACKNOWLEDGEMENTS

The authors would like to thank the German Research Foundation DFG for the support of the depicted research within the Cluster of Excellence "Integrative Production Technology for High-Wage Countries".

REFERENCES

Arntz, K., 2013, Technologie des Mehrachsfräsens von vergütetem Schnellarbeitsstahl, Aachen

Schug, P. et al, 2012, Durchgängige CAx-Prozessketten, Forschung an der Werkzeugbau Akademie, Apprimus, Aachen

Zabel, A., 2010, Prozesssimulation in der Zerspanung, Vulkan-Verlag, Dortmund

Glaeser, G., 1997, Efficient volume-generation during the simulation of NC-milling, *Proceedings of the international workshop on visualization and mathematics'97*, pp 89-106 Springer, Heidelberg

Jerard, R., 1989, Approximate methods for simulation and verification of numerically controlled machining programs. *Visual Computer 5*, pp 329-348

Robert, L., 1987, Discrete simulation of NC machining, *Proceedings of the third Annual Symposium on Computational Geometry*, Ontario

Ayasse, J., 2001, Interactive manipulation of voxel volumes with free-formed voxel tools, *VM 2001*, Stuttgart

Stautner, M., 2005, Simulation und Optimierung der mehrachsigen Fräsbearbeitung, Vulkan Verlag Essen.

CGTech [Online], 2013, *http://cgtech.com*

Meinecke, M., 2009, Prozessauslegung zum fünfachsigen zirkularen Schruppfräsen von Titanlegierungen, Aachen

Diehl A., 2011, Increasing Productivity with Engagement-Generated Toolpaths, *CNC Machining*, Vol 14, Iss 47

Klocke F., 2011, *Manufacturing Processes 1*, Springer, Berlin,

Ståhl, E., 2012, Metal Cutting. *Theories and Models,* Elanders, Lund,

Stifter S., 1995, Simulation of NC Machining Based on the Dexel Model: A Critical Analysis, *Int. Journal for Advanced Manufacturing Technology*, Springer, London

Ren, Y., 2008, Feature Conservation and Conversion of Tri-dexel Volumetric Models to Polyhedral Surface Models for Product Prototyping, *Computer-Aided Design and* Application, CAD Solutions,